

*Publication consideration in **Journal of Electroanalytical Chemistry***

Research Paper

Fluorination effect on electrochemistry of dibutyl viologen in aqueous solution

Tatsuya Ayabe^a, Bun Chan^b, Takamasa Sagara^{b*}

^a*Department of Advanced Technology and Science for Sustainable Development, Graduate School of Engineering, Nagasaki University, Bunkyo 1-14, Nagasaki 852-8521, Japan*

^b*Division of Chemistry and Materials Science, Graduate School of Engineering, Nagasaki University, Bunkyo 1-14, Nagasaki 852-8521, Japan*

ARTICLE INFO

Keywords:

Fluorination effect; Perfluoroalkyl viologen; Redox potential; Diffusion coefficient; DFT calculation

*Corresponding author.

E-mail address: sagara@nagasaki-u.ac.jp (T. Sagara)

Highlight

- Electrochemistry of a new water-soluble perfluoroalkyl viologen was studied.
- FC4VFC4 exhibits less negative E° and smaller D_{ox} than dibutyl viologen.
- DFT calculations unveiled the extents of electron-withdrawing effects.

ABSTRACT

We have synthesized a perfluoro analog of dibutyl viologen by replacing the side $-(\text{CH}_2)_2\text{-CH}_2\text{CH}_3$ groups with $-(\text{CH}_2)_2\text{-C}_2\text{F}_5$ groups. The effect of fluorination on the aqueous solution electrochemistry was investigated using experimental voltammetric measurements and DFT computations. The formal potential of one-electron transfer redox couple, viologen radical monocation/dication, became 128 mV less negative upon fluorination, and the diffusion coefficient of the oxidized form was lowered by ca. 12%. Calculations indicated that the shift of the formal potential is largely caused by strong electron-withdrawing nature of the perfluorinated groups despite a separation of $(\text{CH}_2)_2$ from the viologen core. The effect is counter balanced by an opposite but smaller effect from the change of solvation free energy due to perfluorination. This perfluoro viologen is water-soluble in both oxidation states and is expected to be used as a redox probe at electrified oil-water and fluoruous phase-water interfaces.

1. Introduction

Redox reactions of organic electroactive species can be highly sensitive to the micro-environment. In the absence of interfering process such as proton transfer or counter ion binding, properties of the medium can be interpreted from the redox reaction. We can, therefore, use such an electroactive molecule as a probe for the medium. We may probe the chemical micro-environments in organic and inorganic thin films, ionic liquids, metal-organic frameworks, and molecular-assembled structures that are yet to be clarified. Among the most widely used redox cores of the probes are ferrocene and viologen derivatives [1]. As far as their one-electron transfer reactions are concerned, one or both of the oxidation-states of the aromatic redox cores, ferrocenyl and 4,4'-bipyridinium groups, are cationic and show π - π and electrostatic interactions with surrounding molecules. These oxidation-states dependent interactions are also affected by substituents such as side-chain groups. A deeper understanding of the various contributing factors to these interactions would facilitate finer tuning of the redox probe.

Among the various approaches for modifying the redox properties of electroactive species, fluorination of alkyl substituents is an attractive option because of the large electronegativity of the F atom that can substantially change molecular properties. Fluorinated compounds with different degrees of fluorination have been studied to target different properties. For example, partially fluorinated substituents such as $-\text{CH}_2\text{F}$ and $-\text{CF}_3$ groups are frequently utilized for pharmaceuticals for their contrasting binding selectivity, bioavailability, and metabolic stability in comparison with those of their alkyl analogues [2-4]. On the contrary, fully fluorinated alkyl group (perfluoroalkyl group, "Rf") is often used industrially in surfactants to drastically lower critical micellar concentration and surface tension [5].

Perfluoroalkyl surfactants show surface activity for both oil and water [6], but those with long Rf chains (over C8) are not biodegradable due to the high stability associated with the strong C-F bond; the resulting environmental consideration has motivated the development of short Rf chain surfactants [7]. Hasegawa and coworkers provided a

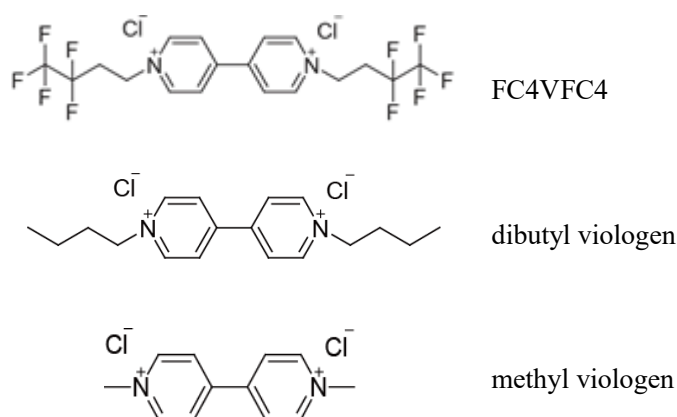
comprehensive account of the properties of Rf compounds on the basis of dipole-dipole interaction of C-F bonds [8]. They proposed that bulk properties of Rf compounds largely emerge from the assembling structures of the Rf molecules. Their infrared spectroscopic analysis showed that a Langmuir-Blodgett film of an amphiphile with a Rf tail longer than $(\text{CF}_2)_9$ is dense and close-packed, whereas that with a Rf tail shorter than $(\text{CF}_2)_6$ is disordered and loose-packed.

In this work, we use viologen to examine the effect of Rf chain on physicochemical characteristics. This choice is based on the specific and desirable properties of viologen such as its reversible and stable one-electron redox activity that are associated with distinct color change. The one-electron reduction product of a viologen dication (V^{2+}), i.e., $\text{V}^{\bullet+}$, has a strong tendency to form a π -stacked dimer $(\text{V}^{\bullet+})_2$. The distinct color differences between V^{2+} , $\text{V}^{\bullet+}$, and $(\text{V}^{\bullet+})_2$ enables the use of UV-visible spectroelectrochemical methods for analysis. When a Rf-chain forms a part of the viologen, it can act as a local probe for, in addition to electrostatic interactions, dipole-dipole attractive interaction between C-F bonds, such as those occurring in perfluorinated anionic surfactant. Our interest lies also in how efficiently a Rf group can withdraw electron from the rather electron-deficient cationic viologen core.

Specifically, we synthesized a new perfluoroalkyl viologen, *N,N'*-di-(1*H*,1*H*,2*H*,2*H*-perfluorobutyl)-4,4'-bipyridinium dichloride (FC4VFC4), as shown in **Scheme 1**, and compare the electrochemistry of this Rf-bearing *water-soluble* viologen with that of the analogous alkyl-bearing viologen counterpart. Water-solubility is a crucial characteristic of this molecule such that it can approach water/oil interface from the aqueous phase. This in turn enables us in future work to use it as a probe for inter-domain environment of a phase-separated polymer such as a Nafion membrane. Singh and Shreeve have synthesized a series of viologen compounds with longer fluoroalkyl chains [9]; however, even their shortest-chain molecule, FC8VFC8, was sparingly soluble in water, precluding aqueous electrochemical characterization. Previously, we synthesized FC6VFC6 diiodide but we found that it is insoluble in water.

We have conducted electrochemical measurements for FC4VFC4 in an aqueous

solution at a Au electrode. We focus on the one-electron transfer process of the $V^{\bullet+}/V^{2+}$ redox couple. We report herein the results of electrochemical measurements at a bare macro Au electrode and an ultra-micro Au electrode in a bulk aqueous medium, as well as insights obtained from our DFT computations.



Scheme 1. Viologen derivatives as chloride salts

2. Experimental

2.1. Material. Water was purified through a Milli-Q Plus Ultrapure water system coupled with an Elix-5 kit (Millipore Co.) to 18.2 M Ω cm. Materials used without further purification include 4,4'-bipyridine (TCI), 1,1,1,2,2-pentafluoro-4-iodobutane (Sigma Aldrich), Nafion 5 wt.% solution (Sigma Aldrich), KCl (Nacalai Tesque), KPF₆ (Sigma Aldrich), tetrabutylammonium chloride (TCI), diethyl ether (EP grade, Nacalai Tesque), acetone (HPLC grade, Nacalai Tesque), and ethanol (HPLC grade, Nacalai Tesque).

2.2. Synthesis. 1,1,1,2,2-Pentafluoro-4-iodobutane (1.70 mmol) was added to *N,N'*-dimethylformamide (DMF) solution of 4,4'-bipyridine (0.71 mmol) at 100°C. After 24 h stirring, an orange precipitate was collected by filtration as the crude product. It was washed by diethyl ether and acetone and dried over silica gel in a desiccator. The

counter anion iodide of the product was exchanged for chloride using an anion exchange resin, Amberlite IR-400. Recrystallization of the white chloride salt from ethanol gave a layered crystal of *N,N'*-di-1*H*,1*H*,2*H*,2*H*-perfluorobutyl-4,4'-bipyridinium dichloride (FC4VFC4 in scheme 1) with a yield of 28.2 %. It was characterized by ¹H NMR, ¹⁹F NMR, and FAB-MS. All the details are listed here: ¹H NMR (300 MHz, DMSO-d₆, TMS ref.): δ = 3.23 (m, 4H), 5.09 (t, 4H), 8.89 (d, 4H), 9.51 (d, 4H); ¹⁹F NMR (400 MHz, DMSO-d₆, HFB ref.): δ = 87.13 (s, 6F), 118.58 (t, 4F); and FAB-MS: m/z calc. for [(deprotonated M²⁺)Cl₂]⁻ 520.23, found 520.2.

N,N'-dibutyl viologen dichloride (C4VC4 in scheme 1), synthesized through the Menshutkin reaction of 4,4'-bipyridine with 1-bromobutane, was subjected to counter anion exchange from iodide to hexafluorophosphate and then to chloride. Home-synthesized methyl viologen dichloride (MV²⁺Cl₂) was also used as a reference compound.

2.3. Electrochemical measurements. All the electrochemical measurements were conducted using either polycrystalline Au electrode with a surface area of 0.021 cm² (BAS Inc.) with a PEEK sheath or an ultra-micro Au electrode (surface area, 74.97 μm², BAS Inc.) with a glass sheath. Voltammetric studies were conducted using a Ag|AgCl|sat'd KCl reference electrode and a coiled Au wire counter electrode. All the potentials in this paper are referenced to a Ag|AgCl|sat'd KCl. All the measurements were performed under an Ar gas (> 99.998%) atmosphere at room temperature (25 ± 2°C).

For the voltammetric measurements, a potentiostat (HECS 326, HUSOU) was employed. The base electrolyte solution in electrochemical measurements was 0.1 M KCl solution unless otherwise stated. Voltammetric studies at the ultra-micro Au electrode (Au-UME) were conducted using a nA-unit head box (HUSOU 972-1).

2.4. Quantum chemistry computations. Standard density functional theory (DFT) computations were carried out with Gaussian 16 [10]. Geometry optimizations and harmonic vibrational frequency calculations were carried out using the N12 method [11]

in conjunction with the 6-31G(d) basis set. Improved single-point energies were calculated with the MN15 functional [12] and the 6-311+G(3df,2p) basis set. Zero-point vibrational energies, thermal corrections to 298 K enthalpies, and 298 K entropies were obtained using N12/6-31(d) frequencies scaled by previously determined scale factors [13]. The effect of aqueous solvation was incorporated using the SMD continuum solvation model [14] using densities calculated with the M05-2X functional [15] together with the 6-31G(d) basis set. Relative energies are reported in kJ mol^{-1} .

3. Results

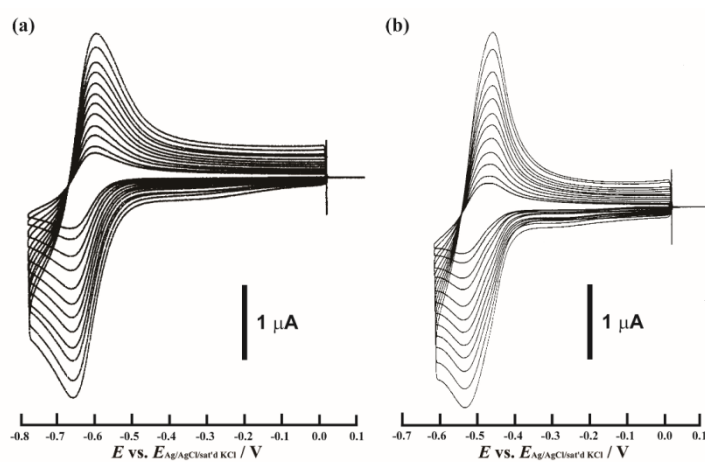


Fig. 1.

3.1. Voltammograms at a macro Au electrode. Voltammograms obtained at a bare 0.021 cm^2 -Au electrode in 0.5 mM aqueous solutions of C4VC4 (**Fig. 1-a**) and FC4VFC4 (**Fig. 1-b**) showed the $\text{V}^{\bullet+}/2^+$ redox reactions. Both viologens exhibited redox processes of solution phase species largely controlled by diffusion with no apparent trace of the redox process of adsorbed species. It is known that $\text{V}^{\bullet+}$ tends to dimerize [16]; our UV-vis spectroscopic measurements for a 0.5 mM solution of $\text{FC4V}^{\bullet+}\text{FC4}$ in the presence of excess dithionite showed that $\text{FC4V}^{\bullet+}\text{FC4}$ dimer constitutes less than 4% of the total $\text{FC4V}^{\bullet+}\text{FC4}$ population. We took the formal potential, $E^{\circ'}$, for

$V^{\bullet+}$ -monomer/ V^{2+} couple as the midpoint potential (E_m) between the anodic (E_{pa}) and cathodic (E_{pc}) peak potentials at $\nu = 100 \text{ mV s}^{-1}$, giving $E^{\circ} = -648 \text{ mV}$ for C4VC4 and $E^{\circ} = -518 \text{ mV}$ for FC4VFC4.

A small additional cathodic current around -0.3 V originated from reduction of residual oxygen. We did not take further efforts to remove oxygen, because this level of cathodic current never affected our analysis of the solution phase redox of viologens.

The peak separation, ΔE_p , for C4VC4 was 61 mV in the range of ν from 10 to 200 mV s^{-1} , and ΔE_p for FC4VFC4 was 66 mV from 15 to 200 mV s^{-1} . When ν was lowered to 2 mV s^{-1} , ΔE_p for FC4VFC4 was 57 mV . For both viologens, the cathodic peak current (i_{pc}) and the anodic peak current (i_{pa}) were equal at any given ν , and they were proportional to $\nu^{1/2}$. Because the voltammetric features are of one-electron transfer reversible response, we used Eq. (1) to obtain diffusion coefficients [17]:

$$i_{pc} = -(2.69 \times 10^5) n^{3/2} A D_{ox}^{1/2} \nu^{1/2} C_{ox}^* \quad (1)$$

where i_{pc} is given in the unit of A, $n = 1$ is the number of electron involved in the redox reaction, A is the surface area of the electrode in cm^2 , D_{ox} is the diffusion coefficient of V^{2+} in $\text{cm}^2 \text{ s}^{-1}$, ν is given in V s^{-1} , and C_{ox}^* is the bulk concentration of viologen in mol cm^{-3} . The D_{ox} values for C4VC4, $4.51 \times 10^{-6} \text{ cm}^2 \text{ s}^{-1}$, and FC4VFC4, $3.85 \times 10^{-6} \text{ cm}^2 \text{ s}^{-1}$, were obtained from the slopes of $i_{pc}-\nu^{1/2}$ plots, assuming that the effect of electrode surface roughness was negligible.

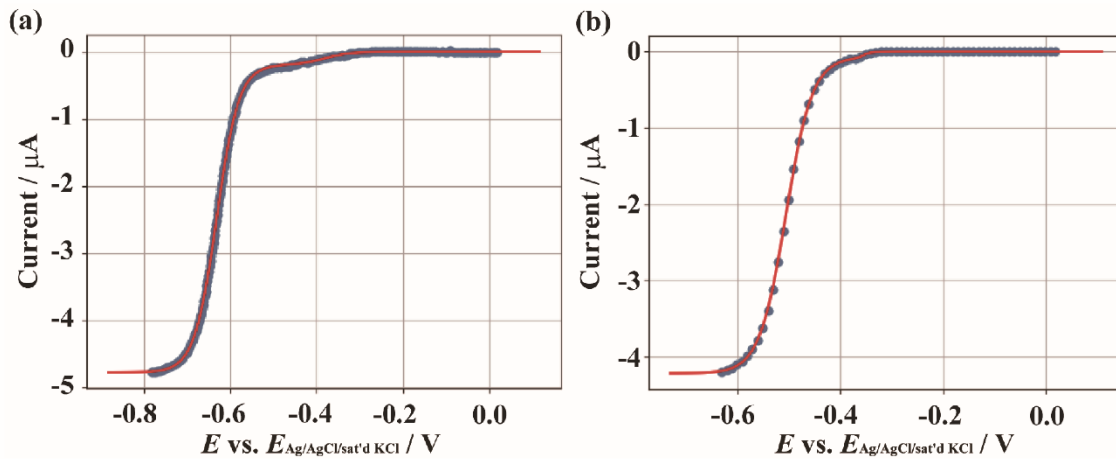


Fig. 2.

3.2. *Voltammograms at a Au-UME.* Steady-state voltammograms were measured at a Au-UME to evaluate the diffusion coefficients. The steady-state limiting current is described by Eq. (2) [18]:

$$i_{\text{lim}} = 4nF C_{\text{ox}}^* D_{\text{ox}} r \quad (2)$$

where r is the radius of a circular UME. The steady-state CVs were recorded at $\nu = 1$ mV s⁻¹, and the resulting data were fitted to Eq. (3), which includes a constant residual current term a , the Nernstian current-potential curve of the reduction of viologen, and an additive third term representing oxygen reduction current.

$$i(E) = a - \frac{i_{\text{lim}}}{1 + \exp\left[\frac{nF(E - E^0)}{RT}\right]} - \frac{i_c}{1 + \exp\left[\frac{bF(E - E_c)}{RT}\right]} \quad (3)$$

In the non-linear regression fitting, $n = 1$ was set. The red lines in **Fig. 2** are the fitted ones with optimal parameters $a(\text{C4VC4}) = 6.0 \times 10^{-13}$ A and $a(\text{FC4VFC4}) = 6.9 \times 10^{-15}$ A, $i_{\text{lim}}(\text{C4VC4}) = 4.59 \times 10^{-10}$ A, $i_{\text{lim}}(\text{FC4VFC4}) = 4.15 \times 10^{-10}$ A. The best fit parameter i_c was 1.9×10^{-11} A and 7.7×10^{-12} A, respectively, for C4VC4 and FC4VFC4. The values of D_{ox} were then calculated from the fitted values of i_{lim} using Eq. (2).

Table 1 summarizes the values of E^0 and D_{ox} obtained for the two viologens of interest, together with those for methyl viologen (MV). The values of E^0 and D_{ox} obtained from two methods closely agree with one another, whereas D_{ox} values obtained using an UME are greater by 9 – 13 % than those obtained using a macro Au electrode. The difference by ca. $\pm 10\%$ is likely due to the uncertainty of the electrode size after polishing, although the size was calibrated by using the redox reaction of $\text{Ru}(\text{NH}_3)_6^{2+/3+}$ prior to the polishing. Upon fluorination, D_{ox} was lowered by 14% (macro Au) and 10% (UME).

Table 1. Formal potentials and diffusion coefficients for methyl viologen (MV), C4VC4, and FC4VFC4 obtained from the CV measurements using the macro Au electrode and Au-UME.

	Macro electrode		UME	
	E° [mV]	$10^6 D_{\text{ox}}$ [cm ² s ⁻¹]	E° [mV]	$10^6 D_{\text{ox}}$ [cm ² s ⁻¹]
MV	-626	7.11	-623	7.86
C4VC4	-628	4.51	-631	4.87
FC4VFC4	-498	3.85	-506	4.40

3.3. DFT thermochemistry. The aqueous reduction of a viologen dication (V^{2+}) can be considered as a combination of a sequence of hypothetical reactions, as shown in **Fig. 3**. First, an aqueous V^{2+} and a solvated electron are taken from the solution to the gas phase (reaction 2, desolvation). This is followed by the combination of these two species to give the gas-phase radical monocation $V^{\bullet+}$ (reaction 3, reduction). Finally, bringing the gas-phase reduced species to water (reaction 4, solvation) completes the thermochemical cycle for the overall reaction 1. The computed values for these processes are shown in **Table 2**, with the contributing aqueous solvation free energy for electron (-148.5 kJ mol⁻¹) taken from literature. [19]

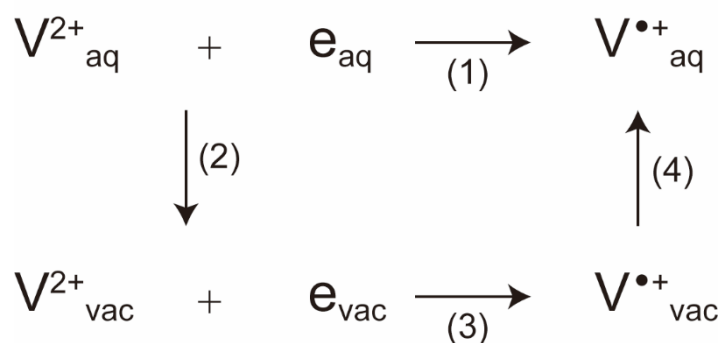


Fig. 3.

Table 2. Computed 298 K free energies (kJ mol⁻¹) for the aqueous reduction of FC4VFC4 (F) and C4VC4 (H) and for their component elementary processes

process		$\Delta G(\text{F})$	$\Delta G(\text{H})$	$\Delta\Delta G(\text{F} - \text{H})$
desolvation	$\text{V}^{2+}_{\text{aq}} + \text{e}_{\text{aq}} \rightarrow \text{V}^{2+}_{\text{vac}} + \text{e}_{\text{vac}}$	844.3	794.8	49.4
reduction	$\text{V}^{2+}_{\text{vac}} + \text{e}^- \rightarrow \text{V}^{\bullet+}_{\text{vac}}$	-895.5	-849.0	-46.5
solvation	$\text{V}^{\bullet+}_{\text{vac}} \rightarrow \text{V}^{\bullet+}_{\text{aq}}$	-191.8	-168.3	-23.5
overall	$\text{V}^{2+}_{\text{aq}} + \text{e}^- \rightarrow \text{V}^{\bullet+}_{\text{aq}}$	-243.1	-222.4	-20.6

As we shall see, another interesting difference between FC4VFC4 and C4VC4 is their aqueous solubilities. Direct quantum chemistry computation of such a quantity is non-trivial. However, one can envisage that, for ionic species, the solvation of an ion pair can serve as a proxy for qualitatively comparing the solubilities of similar species. We have put this into practice by calculating the dissolution of gas-phase $(\text{V}^{n+})(\text{Cl}^-)_n$ to form $\text{V}^{n+}_{\text{aq}}$ and $n \cdot \text{Cl}^-_{\text{aq}}$ via aqueous $(\text{V}^{n+})(\text{Cl}^-)_n$, where $n = 2$ for V^{2+} or $n = 1$ for $\text{V}^{\bullet+}$. The results are shown in [Table 3](#).

Table 3. Computed solvation free energies (kJ mol⁻¹) of gaseous viologen chlorides [FC4VFC4 (F) and C4VC4 (H)] and their energy components

process	$\Delta G(\text{F})$	$\Delta G(\text{H})$	$\Delta\Delta G(\text{F} - \text{H})$
$\text{VCl}_{2,\text{vac}} \rightarrow \text{VCl}_{2,\text{aq}}$	-213.2	-203.8	-9.3
$\text{VCl}_{2,\text{aq}} \rightarrow \text{V}^{2+}_{\text{aq}} + 2 \text{Cl}^-_{\text{aq}}$	-54.1	-67.5	13.4
overall	-267.3	-271.4	4.1
$\text{VCl}_{1,\text{vac}} \rightarrow \text{VCl}_{1,\text{aq}}$	-131.1	-129.4	-1.7
$\text{VCl}_{1,\text{aq}} \rightarrow \text{V}^+_{\text{aq}} + \text{Cl}^-_{\text{aq}}$	-31.5	-38.7	7.3
overall	-162.5	-168.1	5.6

4. Discussion

4.1. Formal potential Difference. The obtained $E^{\circ'}$ values in **Table 1** show small method-to-method deviations that are less than ± 6 mV. The $E^{\circ'}$ value for MV is -624 ± 1 mV (**Table 1**), which compares well with the frequently cited literature values of -643 mV [20] as well as -0.63 V in 0.1 M NaCl [21] and thus further validates our determination. The $E^{\circ'}$ value of C4VC4 is in accord with the typical values of dialkyl viologen dichloride, while the value for FC4VFC4 is approximately 128 mV more positive than that for C4VC4.

The calculated difference of the Gibbs energy change, -20.6 kJ mol⁻¹ (**Table 2**), which corresponds to a more positive redox potential for FC4VFC4 than that for C4VC4, is in qualitative agreement with the experimental difference. Both the desolvation step and the reduction step involve large free energy changes of approximately 800 kJ mol⁻¹. They also contribute substantially to the difference between FC4VFC4 and C4VC4. Coincidentally, the free energy difference of 49.4 kJ mol⁻¹ for the desolvation step is similar in magnitude to that for the reduction step (-46.5 kJ mol⁻¹); the opposite signs of the two steps lead to a cancellation of the energy differences, such that the overall difference of -20.6 kJ mol⁻¹ is similar to the difference for the final solvation processes (-23.5 kJ mol⁻¹).

Intuitively, the difference in the gas-phase reductions of FC4VFC4 and C4VC4 may be a result of two prospective effects, namely (1) direct overlap of the electron-accepting orbitals with the orbitals of the electron-withdrawing substituents, and (2) long-range polarization effect. The latter effect has been proposed by Hünig and Schenk to account for observations that a viologen with strong electron-withdrawing groups show more positive $E^{\circ'}$ than that with weaker electron-withdrawing groups [22]. We have considered both effects. Regarding the effect of orbital overlap, an examination of the (viologen-based) LUMO of FC4VFC4 shows a slight extension of the orbital beyond the viologen core but it does not reach the fluorinated termini. To probe the long-range through-space effect of the C₂F₅ group, we have computed the energies for the reduced forms of FC4VFC4 analogs that contain longer alkyl spacers

$-(\text{CH}_2)_m\text{-C}_2\text{F}_5$.) up to $m = 5$. Even for the molecule with $m = 5$, the energy is still lower than the value for C4VC4. We also find that, intuitively, for the analogs of FC4VFC4 that contain longer alkyl spacers (up to $-(\text{CH}_2)_7\text{-C}_2\text{F}_5$), positive Mulliken charge of bipyridinium unit increases with decreasing separation unit of CH_2 . However, the increase of the positive charge on the bipyridinium unit with the increase of m does not diminish for m up to 7. For $m = 2$ (FC4VFC4, i.e., the system used in our experiment), both the reducing energy and the Mulliken atomic charge indicate that the long-range polarization effect operates between bipyridinium unit and $-\text{C}_2\text{F}_5$ group. Taken together, we can conclude that the long-range polarization effect is dominant for the gas-phase reductions of FC4VFC4 and C4VC4.

We now turn our attention to the desolvation and solvation processes. The calculated free energies suggest a higher hydrophilicity for FC4VFC4 than that for C4VC4. Although our calculations do not provide a breakdown of contributing effects, this result can be rationalized by a greater local dipole moment of the $-\text{C}_2\text{F}_5$ group, which can be inferred from the computed Mulliken atomic charges. The difference for desolvating the dication is larger than that for solvating the monocation, as one would intuitively expect.

Overall, two of the three component processes in the thermochemical cycle of [Fig. 3](#) favor the reduction of FC4VFC4 over that of C4VC4; the strong electron-withdrawing nature of C_2F_5 polarizes the central viologen unit and leads to a more facile intrinsic (gas-phase) reduction for FC4VFC4, and the more polar FC4VFC4 radical monocation solvates better than the less polar C4VC4. These effects overcome the larger energy penalty for desolvating FC4VFC4 dication relative to desolvating C4VC4 dication, as a whole yielding a more favorable aqueous reduction of FC4VFC4.

4.2. Diffusion coefficients. The two methods of measurements both gave smaller D_{ox} for FC4VFC4 than those for C4VC4 by 10-15 %. Estimation of D_{ox} can be made using the Nernst-Einstein equation:

$$D_{\text{ox}} = k_{\text{B}}T/6\pi\eta r_{\text{s}} \quad (4)$$

where k_{B} is the Boltzmann constant, η is the viscosity, r_{s} is the Stokes radius of the particle as approximated by a sphere. Our DFT calculations in the preceding section also provide us with the information regarding the structure of the viologens; for both oxidation states and for both compounds, conformations with extended side chains are more stable than the inward-pointing, bent side chain conformations. This implies that there should be little difference in r_{s} between the two compounds, and the cause of the difference of D_{ox} is by other factors. A potential cause of the smaller diffusion coefficient of perfluoroalkyl viologen is difference in the structures of water clusters surrounding and the highly polar perfluoroalkyl $-\text{C}_2\text{F}_5$ moiety. This possibility will be investigated in future studies.

4.3. Aqueous solubility. The oxidized form of FC4VFC4 is water-soluble, although its saturated concentration was found to be lower than 1 mM. In contrast, C4VC4 has a much higher solubility than FC4VFC4 does. This observation seemingly contradicts the higher hydrophobicity of FC4VFC4 than the hydrophobicity of C4VC4, as discussed in the previous session on the basis of the results of **Table 2**. However, the discussion of solubility should also take the interaction with the counterion into account. Separately, to investigate the effect of the chain length on the solubility, we synthesized 1*H*,1*H*,2*H*,2*H*-perfluorohexyl-4,4'-bipyridinium iodide, and found it to be completely insoluble in water, even though the hydrocarbon analog diheptyl viologen is soluble.

Our DFT Gibbs free energy changes for the process of solvating and ionizing gas-phase $(\text{V}^{2+})(\text{Cl}^-)_2$ and $(\text{V}^{\bullet+})(\text{Cl}^-)$ to give, respectively, $[\text{V}^{2+}_{\text{aq}} + 2\text{Cl}^-_{\text{aq}}]$ and $[\text{V}^{\bullet+}_{\text{aq}} + 2\text{Cl}^-_{\text{aq}}]$ (**Table 3**) are consistent with experimental observation that FC4VFC4 is less soluble than C4VC4. The energies for component elementary steps of the overall dissolution indicate that the fluorinated species are more soluble as ion pairs in comparison with the corresponding ion pairs of the hydrocarbon. However, the stronger binding with the counter ions for FC4VFC4 dominates, which hinders the ionization

step and as a result leads to an overall lower solubility than the non-fluorinated viologen species.

4. Conclusions

We present a detailed investigation of the solution electrochemistry of the perfluorinated viologen (FC4VFC4), which reveals the effect of sidechain fluorination on the physicochemical properties. The oxidized form of FC4VFC4 has a more positive formal potential and a lower diffusion coefficient in water than C4VC4. The positive shift of formal potential E° arose from strong long-range polarization effect of the perfluorinated groups, despite a separation of $(\text{CH}_2)_2$ from the viologen core. Two probable contributing factors to the positive shift are considered: (1) contribution of C_2F_5 unit to the electron-accepting LUMO, and (2) long-range polarization effects of the C_2F_5 unit. Our DFT computations indicate that the latter effect is substantial, with a C_2F_5 unit showing considerable effects on E° for substrates with up to approximately five CH_2 units of separation.

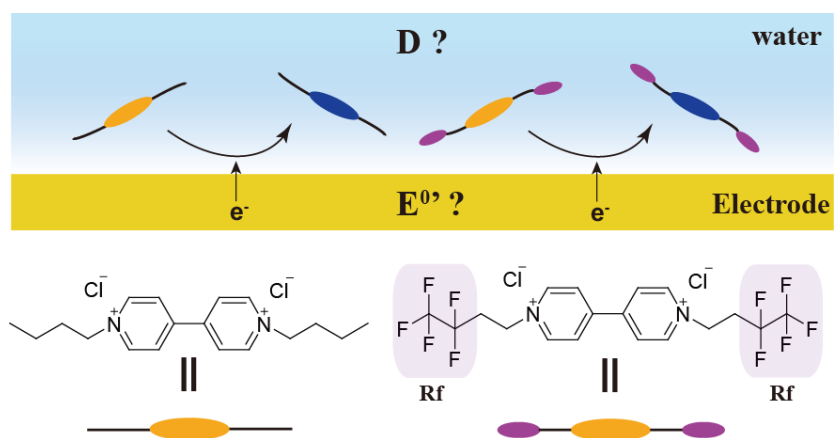
The lower D_{ox} of FC4VFC4 when compared with C4VC4 is not likely to be a result of conformational differences of the two molecules in water. We find that the fluorinated compounds to be generally less soluble in water than their hydrocarbon counterparts. Our calculations suggest that fluorination facilitate solvation of bare ion pair of the viologen and its counter ions. The stronger binding with the counter ions, however, gives rise to a lower solubility than the non-fluorinated viologen species. This is consistent with the report of Hasegawa and coworkers. [8]

Finally, this perfluoro viologen is water-soluble in both oxidation states and is expected to be used as a redox probe at electrified oil-water and fluorous phase-water interfaces.

Acknowledgements

The authors acknowledge with appreciation to Dr. Hironobu Tahara at Nagasaki University for technical advices and useful discussions. This work was supported by a Grant-in Aid for Scientific Research on Innovative Areas “Molecular Engine” (JSPS KAKENHI Grant Number JP19H05400) and a research grant from Izumi Science and Technology Foundation to TS. Generous computational resources are provided (to BC) by RIKEN Information Systems Division (project Q19266).

Graphical abstract



References

[1] A. Moiodek, H. Q. A. Lê, H. S.-Dorizon, H. K.-Youssoufi, Streptavidin-polypyrrole Film as Platform for Biotinylated Redox Probe Immobilization for Electrochemical Immunosensor Application, *Electroanalysis*, 28 (8) (2016) 1824-1832.

<https://doi.org/10.1002/elan.201600139>

[2] M. Shimizu, T. Hiyama, Modern Synthetic Methods for Fluorine-Substituted Target Molecules, *Angew. Chem. Int. Ed.*, 44 (2) (2005) 214-231.

<https://doi.org/10.1002/anie.200460441>

[3] J. Wang, M. Sánchez-Roselló, J. L. Aceña, C. del Pozo, A. E. Sorochinsky, S. Fustero, V. A. Soloshonok, H. Liu, Fluorine in Pharmaceutical Industry: Fluorine-Containing Drugs Introduced to the Market in the Last Decade (2001–2011), *Adv. Mater.*, 114 (4) (2014) 2432-2506.

<https://doi.org/10.1021/cr4002879>

[4] X. Shao, C. Xu, L. Lu, Q. Shen, Shelf-Stable Electrophilic Reagents for Trifluoromethylthiolation, *Acc. Chem. Res.*, 48 (5) (2015) 1227-1236.

DOI: [10.1021/acs.accounts.5b00047](https://doi.org/10.1021/acs.accounts.5b00047)

[5] M. M. Schultz, D. F. Barofsky, J. A. Field, Fluorinated Alkyl Surfactants, *Environ. Eng. Sci.*, 20 (5) (2003) 487-499.

<https://doi.org/10.1089/109287503768335959>

[6] B. Arkles, Barry, Y. Pan, Youlin, Y. M. Yun, The Role of Polarity in the Structure of Silanes Employed in Surface Modification, Chap. 10, in: K. L. Mittal, (Ed.), *Silanes and Other Coupling Agents*, Vol. 5, Koninklijke Brill NV, Leiden (2009) 51-64.

[10.1163/ej.9789004165915.i-348.37](https://doi.org/10.1163/ej.9789004165915.i-348.37)

[7] P. J. Huang, M. Hwangbo, Z. Chen, Y. Liu, J. Kameoka, K.-H. Chu, Reusable Functionalized Hydrogel Sorbents for Removing Long and Short-Chain Perfluoroalkyl Acids (PFAAs) and GenX from Aqueous Solution, *ACS Omega*, 12 (3) (2018) 17447-17455.

<https://doi.org/10.1021/acsomega.8b02279>

- [8] T. Hasegawa, Physicochemical Nature of Perfluoroalkyl Compounds Induced by Fluorine, *Chem. Rec.*, 17 (10) (2017) 903-917.
<https://doi.org/10.1002/tcr.201700018>
- [9] R. P. Singh, J. M. Shreeve, Syntheses of the first N-mono- and N,N'-dipolyfluoroalkyl-4,4-bipyridinium compounds, *Chem. Commun.*, (2003) 1366-1367.
<https://doi.org/10.1039/B301968C>
- [10] M. J. Frisch, G. W. Trucks, H. B. Schlegel, G. E. Scuseria, M. A. Robb, J. R. Cheeseman, G. Scalmani, V. Barone, G. A. Petersson, H. Nakatsuji, X. Li, M. Caricato, A. V. Marenich, J. Bloino, B. G. Janesko, R. Gomperts, B. Mennucci, H. P. Hratchian, J. V. Ortiz, A. F. Izmaylov, J. L. Sonnenberg, D. Williams-Young, F. Ding, F. Lipparini, F. Egidi, J. Goings, B. Peng, A. Petrone, T. Henderson, D. Ranasinghe, V. G. Zakrzewski, J. Gao, N. Rega, G. Zheng, W. Liang, M. Hada, M. Ehara, K. Toyota, R. Fukuda, J. Hasegawa, M. Ishida, T. Nakajima, Y. Honda, O. Kitao, H. Nakai, T. Vreven, K. Throssell, J. A., Jr. Montgomery, J. E. Peralta, F. Ogliaro, M. J. Bearpark, J. J. Heyd, E. N. Brothers, K. N. Kudin, V. N. Staroverov, T. A. Keith, R. Kobayashi, J. Normand, K. Raghavachari, A. P. Rendell, J. C. Burant, S. S. Iyengar, J. Tomasi, M. Cossi, J. M. Millam, M. Klene, C. Adamo, R. Cammi, J. W. Ochterski, R. L. Martin, K. Morokuma, O. Farkas, J. B. Foresman, D. J. Fox, *Gaussian 16 Revision B.01*, Gaussian, Inc., Wallingford, CT, 2016.
- [11] R. Peverati, D. G. Truhlar, Exchange-Correlation Functional with Good Accuracy for Both Structural and Energetic Properties while Depending Only on the Density and Its Gradient, *J. Chem. Theory Comput.*, 7 (8) (2012) 2310-2319.
<https://doi.org/10.1021/ct3002656>
- [12] H. S. Yu, X. He, S. L. Li, D. G. Truhlar, MN15: A Kohn-Sham Global-Hybrid Exchange-Correlation Density Functional with Broad Accuracy for Multi-Reference and Single-Reference Systems and Noncovalent Interactions, *Chem. Sci.*, 7 (8) (2016) 5032-5051.
<https://doi.org/10.1039/c6sc00705h>

[13] B. Chan, Use of Low-Cost Quantum Chemistry Procedures for Geometry Optimization and Vibrational Frequency Calculations: Determination of Frequency Scale Factors and Application to Reactions of Large Systems, *J. Chem. Theory Comput.*, 12 (13) (2017) 6052-6060.

<https://doi.org/10.1021/acs.jctc.7b00721>

[14] A. V. Marenich, C. J. Cramer, D. G. Truhlar, Universal Solvation Model Based on Solute Electron Density and a Continuum Model of the Solvent Defined by the Bulk Dielectric Constant and Atomic Surface Tensions, *J. Phys. Chem. B*, 18 (113) (2009) 6378-6396.

<https://doi.org/10.1021/jp810292n>

[15] Y. Zhao, N. E. Schultz, D. G. Truhlar, Design of Density Functionals by Combining the Method of Constraint Satisfaction with Parametrization for Thermochemistry, Thermochemical Kinetics, and Noncovalent Interactions, *J. Chem. Theory Comput.*, 2 (2) (2006) 364-382.

<https://doi.org/10.1021/ct0502763>

[16] E. M. Kosower, J. L. Cotter, Stable Free Radicals. 11. The Reduction of 1-Methyl-4-cyanopyridinium Ion to Methylviologen Cation Radica, *J. Am. Chem. Soc.*, 86 (24) (1964) 5524-5527.

<https://doi.org/10.1021/ja01078a026>

[17] A.J. Bard, L.R. Faulkner, *Electrochemical Methods—Fundamentals and Applications*, 2nd ed., John-Wiley & Sons, New York, 2001, Chap. 12.

[18] Y. Saito, A Theoretical Study on the Diffusion Current at the Stationary Electrodes of Circular and Narrow Band Types, *Rev. Polarogr.*, 15 (6) (1968) 177-187.

<https://doi.org/10.5189/revpolarography.15.177>

[19] C.-G. Zhan, D. A. Dixon, The Nature and Absolute Hydration Free Energy of the Solvated Electron in Water, *J. Phys. Chem. B* 18 (107) (2003) 4403-4417.

<https://doi.org/10.1021/jp022326v>

[20] L. Michaelis, E. S. Hill, *J. Gen. Physiol.* 16 (6) (1933) 859-873.

<https://doi.org/10.1085/jgp.16.6.859>

[21] T. Janoschka, N. Martin, M.D. Hager, U.S. Schubert, An Aqueous Redox-Flow Battery with High Capacity and Power: The TEMPTMA/MV System, *Angew. Chem. Int. Ed.* 55 (46) (2016) 14427-14430.

<https://doi.org/10.1002/anie.201606472>

[22] S. Hünig, W. Schenk, *Liebigs Ann. Chem.*, 10 (1979) 1523-1533.

<https://doi.org/10.1002/jlac.197919791011>

Figure captions

Fig. 1. CVs of a bare macro-Au electrode ($A = 0.201\text{cm}^2$) in (a) 0.5 mM C4VC4 + 0.1 M KCl solution and (b) 0.5 mM FC4VFC4 + 0.1 KCl solution. For both (a) and (b), $\nu = 200, 170, 140, 120, 100, 80, 65, 50, 35, 25, 15, 10\text{ mV s}^{-1}$.

Fig. 2. CVs of the Au-UME ($A = 74.97\text{ }\mu\text{m}^2$) recorded at $\nu = 1\text{ mVs}^{-1}$ in a 0.5 mM C4VC4 + 0.1 M KCl solution (a) and in a 0.5 mM FC4VFC4 + 0.1 M KCl solution (b). Blue circles are experimental data; whereas red curves are the best fit results.

Fig. 3. Representation of aqueous reduction of a viologen dication (V^{2+}) using combination of a sequence of hypothetical reactions. For reactions (1) through (4), see text.

Graphical abstract

